

## INFLUENCE ON THE QUALITY OF SECONDARY ALUMINUM ALLOY CASTS BY Mn ADDITION

doi: 10.2478/cqpi-2019-0043

Date of submission of the article to the Editor: 11/03/2019

Date of acceptance of the article by the Editor: 27/05/2019

**Lenka Kuchariková**<sup>1</sup> – *orcid id: 0000-0002-2688-1075*

**Eva Tillová**<sup>1</sup> – *orcid id: 0000-0002-1010-0713*

**Magdalena Mazur**<sup>2</sup> – *orcid id: 0000-0003-3515-8302*

**Adrián Herčko**<sup>1</sup>

<sup>1</sup>University of Žilina, Faculty of Mechanical Engineering, **Slovakia**

<sup>2</sup>Czestochowa University of Technology, Faculty of Management, **Poland**

**Abstract:** The quality of aluminum casts is necessary in order to reach sufficient properties required for application. The decreasing in the properties of aluminum cast mainly related with microstructure, especially with size and morphology of second phases. One of such second phases in aluminum alloys are the  $\beta$ -phases. These phases are unwanted mainly because of the decreasing of mechanical properties. The contribution is deal with influence of addition of Mn to affecting the formation of  $\beta$ -phases in the AlSi7Mg0.3 and AlSi7Mg0.6 cast alloys. These materials are used for application especially automotive industry. The results shows, that addition of Mn is not sufficient for affecting of formation of the Fe-rich phases in AlSi7Mg0.6 cat alloys, but in the AlSi7Mg0.3 this addition lead to changes in formation of Fe-rich intermetallic phases.

**Keywords:** secondary aluminum alloys, intermetallic phases, addition of Mn, quality of casts

### 1. INTRODUCTION

While secondary aluminum alloys are beneficial for practical, economical, and ‘carbon-footprint’ points of view, their increased iron content is still the key obstacle to a widespread use in casting applications which require high ductility (Bosch et al., 2014). The detrimental effect of  $\beta$ -Al<sub>5</sub>FeSi intermetallics phases on the mechanical properties of Al-Si alloys is well known and therefore the iron content is strictly limited. The high iron contents lead to formation of very large Fe-rich needles and can extend up to several millimeters in length. Therefore, it is necessary to known that under normal casting conditions and with moderate Fe levels, these intermetallics grow more typically in the size range of 50 – 500  $\mu$ m. In castings with very high cooling rates and/or when using low Fe levels (e.g. primary alloy ingot), the intermetallic particles are typically of the order of 10 - 50  $\mu$ m (Bosch et al., 2014; Shabestari, 2004; Taylor, 2012).

The prevention for avoiding to formation of  $\beta$ -Al<sub>5</sub>FeSi intermetallics phases by increasing the cooling rate, superheating the molten metal, or by the adding "iron correctors" = "neutralizer" like Mn, Co, Cr, Ni, V, Mo and Be. For large-scale industrial usage, the Fe correction with Mn is accepted as the preferred economical solution due to its easy and uncritical implementation, and its relatively low price compared to other potential neutralizers. In addition, manganese helps to prevent die soldering during processing. Excess Mn may reduce Al<sub>5</sub>FeSi phase and promote formation Fe-rich phases Al<sub>15</sub>(FeMn)<sub>3</sub>Si<sub>2</sub> (know as alpha- or  $\alpha$ -phase) in form „skeleton like“ or in form „Chinese script“ (Bosch et al., 2014; Shabestari, 2004; Taylor, 2012; Bidmeshki et al., 2016). The size and amount of Al<sub>5</sub>FeSi also contribute to the formation of solidification defects, such as porosity and hot tearing (Puncreobutr et al., 2014). The commonly used assessment of such dimensions are quantitative image analysis (Vaško, 2016; Bilewicz et al., 2013; Belan, 2014, Zatkalíková, 2017). These methods provide numerical and accurate values of microstructural features. The critical iron content (in wt. %) for an alloy can be calculated using (1) (Rana et al., 2012; Taylor, 2004):

$$Fe_{crit} \approx 0.075 \times [\%Si] - 0.05. \quad (1)$$

If the iron content exceeds 0.45 wt.%, it is reported that the manganese content should not be less than half of the iron. The addition of Mn to melts with high iron levels can also promote the formation of sludge, if the sludge factor (derived by  $[\%Fe] + 2[\%Mn] + 3[\%Cr]$ ) exceeds a particular value for a given alloy and melt holding temperature. This is a serious problem for die-casters who use low melt temperatures and high impurity secondary alloys (Rana et al., 2012; Shabestari, 2004; Taylor, 2004 and 2012). Excess amounts of Mn, however, deteriorate the mechanical properties by increasing the total amount of iron-containing intermetallic phases (Hwang, 2007). Therefore, it is important to study how Mn addition affected the formation of Fe-rich needles and so influence the properties of Al-Si castings.

## 2. METHODOLOGY OF RESEARCH

The bars (with dimension 300 x 20 mm) from experimental alloys were produced by the gravity casting technique and casted into the sand mold in company Uneko Ltd., Zátor, Czech Republic. The experimental bars were made from aluminum scrap of AlSi7Mg alloys. The aim of casting was to produce bars from two typical secondary aluminum cast alloys: AlSi7Mg0.3 (alloy A) and AlSi7Mg0.6 (alloy B) with higher content of Fe about 0.45 wt. % and different Mn contents (alloy A<sup>+Mn</sup> and B<sup>+Mn</sup>) for evaluation of Mn effect to changes of size and area fraction of microstructural features (especially: porosity and Fe-rich phases). The chemical composition of these experimental materials was quantified using spectroscopy analysis on SPECTROMAXx and is shown in Table 1.

The metallography observations of morphology and dimensions of microstructural features changes, due to the effect of Mn addition, was done by using an optical microscope (SDAS factor, are size of pores and Fe-rich phases in form of skeleton-like, length of Fe-rich needles phases, and area fraction of each microstructural features). The samples were prepared by standard metallographic procedures. The SDAS factor was measured using the segment length 12 cm and the number of dendrites salient was calculated. For calculation was used the formula (2) (Djurdjevič et al. 2012, Foundry lexicon).

$$\text{SDAS} = L/(n \cdot M) \quad (2)$$

where: L - length of segment; n - the number of dendrites salient; M - magnification

Table 1

The chemical composition of experimental alloys, wt. %

Alloy	Si	Fe	Cu	Mn	Mg	Zn	Cr	Pb	Ti	Al
A	7.34	0.454	0.021	0.009	0.302	0.02	0.002	0.005	0.118	balance
A <sup>+Mn</sup>	7.051	0.45	0.021	0.122	0.258	0.016	0.002	0.005	0.112	balance
B	7.097	0.429	0.013	0.044	0.466	0.002	0.002	0.005	0.119	balance
B <sup>+Mn</sup>	6.881	0.29	0.011	0.149	0.596	0.002	0.003	0.005	0.103	balance

For the quantitative analysis of area size, length and area fraction of microstructural features, the NIS Elements software with camera Nikon digital sight DS-U2 was used. The results of quantitative analysis represent the average values of the measured data for each measured dimensions.

### 3. RESULTS AND DISSCUSION

#### 3.1. Metallography observation

The microstructure of experimental materials correlate with binary phase diagram of Al-Si system and consists of the solid solution of Si in Al - matrix - dendrites of the  $\alpha$ -phase, eutectic (a mechanical mixture of eutectic Si and  $\alpha$ -phase) and intermetallic phases different chemical compositions (Fig. 1).

Methods used for identification of intermetallic phases in the microstructure of experimental materials (Fig.1) confirmed the occurrence of Fe- and Mg-rich phases:  $\text{Al}_5\text{FeSi}$  (needles-like form),  $\text{AlFeMgSi}$  (skeleton-like form or script-like form), and  $\text{Mg}_2\text{Si}$  (script-like form).

The alloy A have more visible the great  $\text{Mg}_2\text{Si}$  phases particles and Fe-rich phases in form skeleton-like than in others experimental alloys (Fig. 1). After addition of Mn these above mentioned phases were observed in form smaller and fragmented particles (Fig. 1a,b).

The greater content of phases in form skeleton-like and script-like were observed in alloy B (Fig. 1c). After addition of Mn (alloy B<sup>+Mn</sup>) were observed longer phases in form skeleton-like (Fig. 1d). The formation of needles phases in both experimental materials in as-cast state correlate with the less content of Mn in materials (alloy A and B). The producer did not comply the condition of higher manganese content than half of the iron (table 1). After addition of Mn (alloy A<sup>+Mn</sup> and B<sup>+Mn</sup>) phases in form needles were coarsened (Fig. 1b, d) comparison to alloys in as-cast state. The metallography assessment shows that alloy A have a larger phases comparison to alloy B. The opposite effect was recorded for alloys after addition of Mn when alloy A<sup>+Mn</sup> have smaller phases comparison to alloy B<sup>+Mn</sup>.

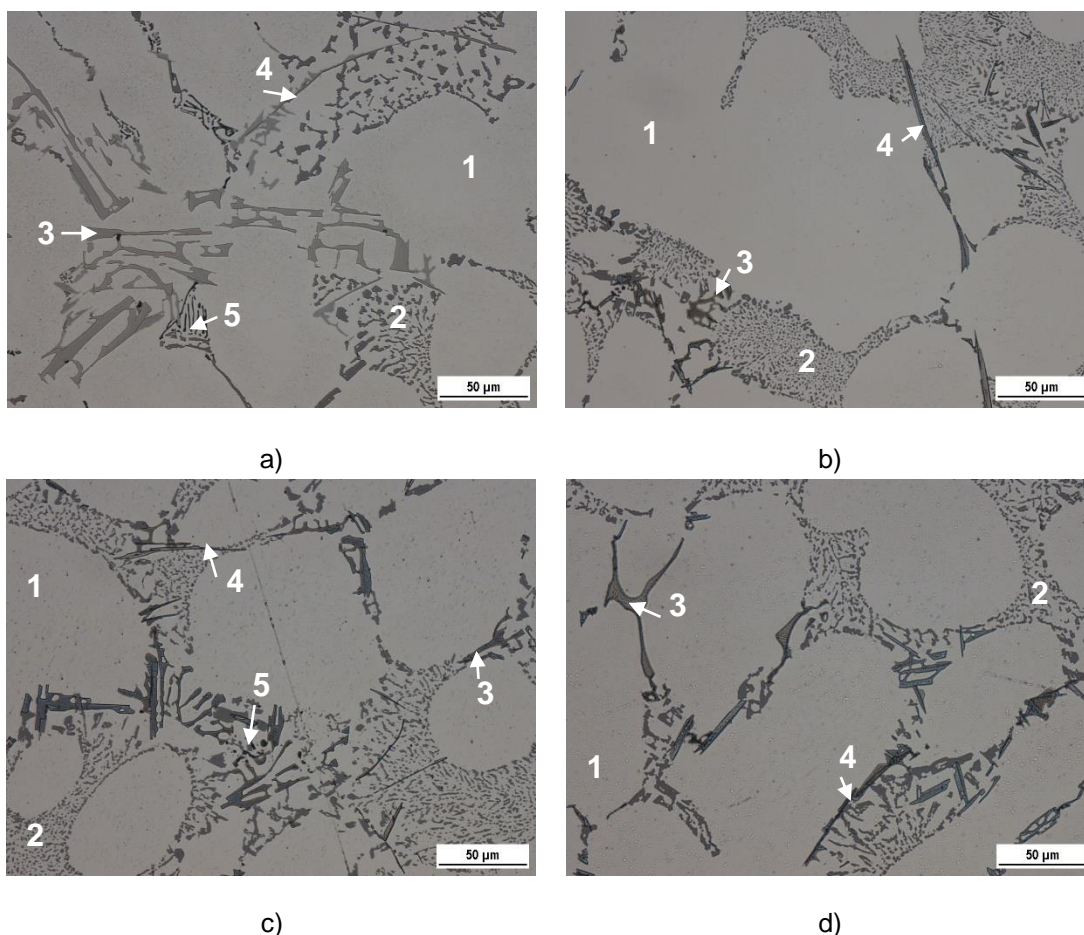


Fig. 1. The microstructure of experimental alloys, etch.  $H_2SO_4$

a) Alloy A; b) Alloy  $A^{+Mn}$ ; c) Alloy B; d) Alloy  $B^{+Mn}$

1-matrix; 2-eutectic; 3-Fe skeleton-like phases; 4-Fe needles phases; 5- $Mg_2Si$

### 3.2. Quantitative analysis

The quantitative analysis of area fraction of microstructural features shows different results for both experimental materials (Fig. 2). The alloys A have the same area fraction of porosity and decreasing area fraction of both Fe-rich phases. The addition of Mn lead to decreasing amount of Fe-rich needles, but the great decreasing was observed also for Fe-rich skeleton-like phases which correlate with small amount of Mn. It can be stated that decreasing amount of Fe-rich phases will lead to better mechanical properties. The quantitative assessment of area fraction of alloy B for both state shows different changes. Despite the requirement of half the Mn (table 1) content the materials after Mn addition shows increasing content of Fe-rich phases. The porosity area fraction was decreasing. These changes will probably lead to decreasing properties such materials.

The assessment of area size and length of microstructural features shows that secondary dendrite arm spacing (SDAS) factor is similar for each experimental materials (Fig. 3). The area size of porosity have increasing tendency. The lowest is in alloy A and the highest in alloy  $B^{+Mn}$ . The difference represents 92.1% lower area size in alloy A (Fig. 3).

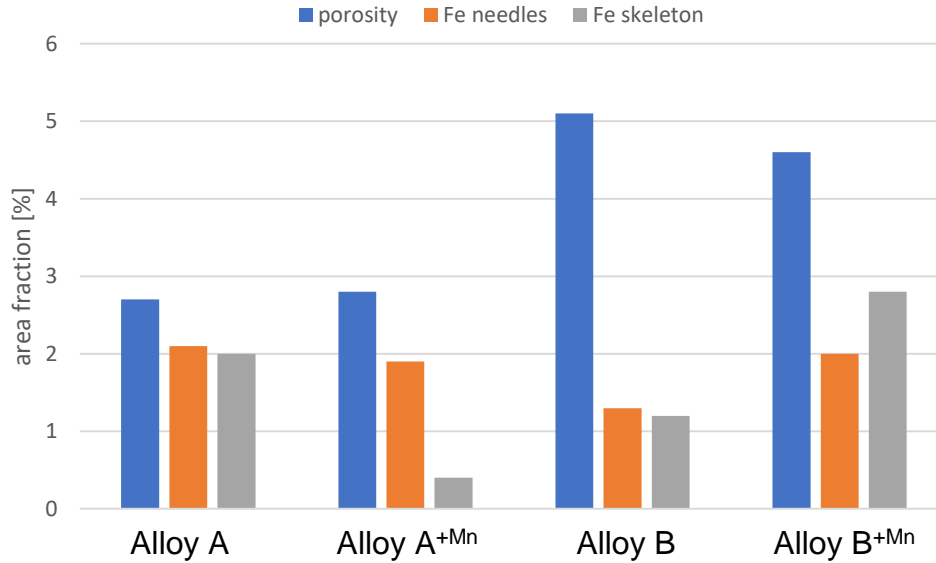


Fig. 2. The results of quantitative analysis (area fraction) of experimental alloys

The length of Fe-rich needles is decreasing with using Mn addition for both experimental alloys (Fig. 3). The length in alloy A<sup>+Mn</sup> was decreasing of about 28 % comparison to alloy A. In material B<sup>+Mn</sup> is decreasing of about 27 % comparison to alloy B. Also it can be written that material A has lower length of these phases than alloy B in both states (without and with addition of Mn). The assessment of area size of Fe-rich phases in from skeleton-like shows that in alloy A decrease their area size from 104  $\mu\text{m}^2$  (for alloy A) to 70.6  $\mu\text{m}^2$  (for alloy A<sup>+Mn</sup>). In alloy B the addition of Mn leads to increasing area size of these phases from 113.6  $\mu\text{m}^2$  (for alloy B) to 266  $\mu\text{m}^2$  (for alloy B<sup>+Mn</sup>). This quantitative assessment shows that the material A in as-cast state or in state after addition of Mn will probably have better properties as material B, in spite of the fact that alloy A does not have the respected ratio of Mn:Fe = 0.5, but alloy B has this ratio.

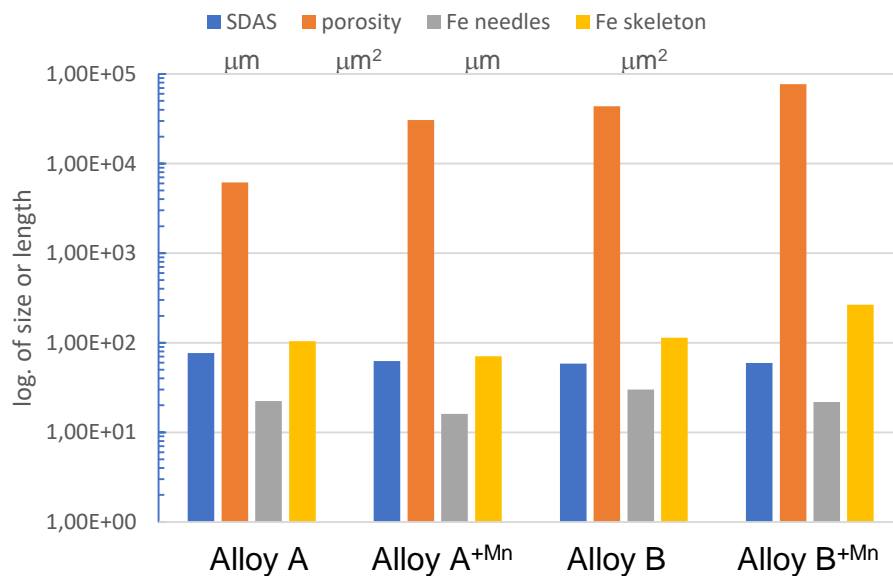


Fig. 3. The results of quantitative analysis (area size, length) of experimental alloys

#### 4. CONCLUSION

The results of assessment of Mn addition influence to the quality of secondary aluminum alloys reflected:

- The metallography observation shows that alloy A have the largest secondary phases (Fe-rich phases) and the eutectic is coarsened, too. The alloy A<sup>+Mn</sup> has the finest morphology of all microstructural features comparison to other experimental alloys.
- The quantitative analysis shows that the lowest length of Fe-rich needles phases and area size of Fe-rich skeleton-like phases, also are fraction of both phases are in alloy A<sup>+Mn</sup>.

The study shows that alloy A<sup>+Mn</sup> have the vest size and morphology of secondary phases. The porosity (area fraction and size) is the smallest in alloy A. therefore can by assumed that better mechanical properties have alloy A and the Mn addition lead to formation of optimal microstructure.

#### ACKNOWLEDGEMENTS

This work has been supported by The Scientific Grant Agency of the Ministry of Education, Science and Sports of the Slovak Republic Academy of Science N° 1/0398/19, N° 012ŽU-4/2019 and N° 049ŽU-4/2017.

(space)

#### REFERENCES

- Belan, J. 2014. *Quantitative Evaluation of alitize coating on ZS6K Ni-base sepealloy*. Metallography XV, Materials science forum, 782, 578-583.
- Bidmeshki, C., Abouei, V., Saghafianb, H., Shabestari, H.G., Noghani, M.T. 2016. *Effect of Mn addition on Fe-rich intermetallics morphology and dry sliding wear investigation of hypereutectic Al-17.5%Si alloys*. Journal of Materials Research and Technology, 5/3, 250-258.
- Bilewicz, M., Palček, P., Tansky, T., Markovičová, L. 2013. *Computer aided image analysisi of nanocomposites*. Archives of Materials Science and Engineering, 64/ 2, 192-197.
- Bösch, D., Pogatscher, A., Hummel, M., Fragner, W., Uggowitzner, P.J., Göken, M., Höppel, H.W. 2014. *Secondary Al-Si-Mg High-pressure Die Casting Alloys with Enhanced Ductility*. Metallurgical and Materials Transactions A, 46/3, 1-11.
- Djurdjevič, M.B., Grzničin, M.A. 2012. *The effect of major alloying elements on the size of the secondary dendrite arm spacing in the as-cast Al-Si-Cu alloys*. Archives of Foundry engineering, 12/1, 19-24.
- Foundry Lexikon, Dendrite arm spacing, Available at: <https://www.giessereilexikon.com/en/foundry-lexikon/Encyclopedia/show/dendrite-arm-spacing-4536/?cHash=2270da0cb276b83fb18fdb72cf4ea2f8>
- Hwang, J. Y., Doty, H.W., Kaufman, M. J. 2007. *The effects of Mn additions on the microstructure and mechanical properties of Al-Si-Cu casting alloys*. Materials Science and Engineering A 488, 496-504
- Rana, R.S., Purohit, R., Das, S. 2012. *Reviews on the influence of alloying elements on the microstructure and mechanical properties of aluminum alloys and aluminum alloy composites*. International Journal of Scientific and research publications, 2/6, 1-7.

- Puncreobutr, C., Phillion, A.B., Fife, J.L., Rockett T.P., Horsfield, A.P., Lee, P.D. 2014. *In situ quantification of the nucleation and growth of Fe-rich intermetallic during Al alloy solidification*. Acta Materialia, 79, 292-303.
- Shabestari, S.G. 2004. *The effect of iron and manganese on the formation of intermetallic compounds in aluminum-silicon alloys*. Materials Science and engineering A 383/2, 289-298.
- Taylor, J.A. 2004. *The Effect of Iron in Al-Si Casting Alloys*. Cooperative Research Centre for Cast Metals Manufacturing (CAST). The University of Queensland Brisbane, Australia, 1-10.
- Taylor, J.A. 2012. *Iron-containing intermetallic phases in Al-Si based casting alloys*. Procedia Materials Science, 1, 19-33.
- Vaško, A. 2016 Evaluation of shape of graphite particles in cast irons by shape factor. Materials Today-proceedings. 3 / 4, 1199-1204.
- Zatkalíková, V., Oravcová, M. Palček, P., Markovičová, L. 2017. *The effect of surface treatment on corrosion resistance of austenitic biomaterial*. Transactions of Famena, 41/4, 25-34.